Spatial Deformation Models for Non-Stationary Max-Stable Processes

Abstract

Max-stable processes constitute the natural class for modeling spatial extremes, but existing models almost all assume spatial stationarity, an assumption rarely verified in practice. This paper proposes a generalization of max-stable processes to the non-stationary framework using the spatial deformation technique. We develop a rigorous theoretical framework based on a generalization of de Haan's spectral representation, enabling the construction of non-stationary max-stable processes from deformed stationary processes. We prove a fundamental characterization theorem: a max-stable process is non-stationary by deformation if and only if there exists a bijective transformation rendering it stationary, and we establish identifiability properties guaranteeing that the deformation is identifiable up to an isometry. Three classes of parametric deformations (piecewise affine, radial, and spline-based) are proposed, and we study the asymptotic properties of the extremal coefficient as well as consistent estimation methods. This work, complementary to the recent algorithmic approach of Richards and Wadsworth (2021), establishes the necessary mathematical foundations for modeling non-stationary extremes in climatology, hydrology, and epidemiology.

Keywords: Max-Stable Processes, Non-Stationarity, Spatial Deformation, Spectral Representation, Spatial Extremes, Identification, Estimation

2010 Mathematics Subject Classification: 60G70, 62H11, 62G32, 62G05, 86A32.

1 Introduction

Max-stable processes play a fundamental role in the statistics of spatial extremes, analogous to that of Gaussian processes for the study of average phenomena. Since the foundational work of [1] on the spectral representation, several operational models have been developed: the storm model of [2], the extremal Gaussian process of [3], and the Brown-Resnick model generalized by [4]. Recent applications of these models to environmental data include the characterization of extreme rainfall

under changing climate [17] and flood risk assessment [18]. Despite these advances, a restrictive hypothesis common to these models is spatial stationarity, rarely verified in practice because altitude, proximity to oceans, or urbanization modify extremal dependence patterns, and ignoring this non-stationarity leads to estimation biases and unreliable predictions [7, 8].

Faced with this observation, the spatial deformation technique, initially introduced by [7] for Gaussian processes, offers an elegant approach to handle non-stationarity by transforming the physical space into a deformed space where the process becomes stationary. This method has recently been extended to the spatial extremes framework by [5], who proposed an algorithmic approach based on least squares minimization of empirical extremal dependence measures. More recently, [16] have developed deep spatial deformation models to capture complex non-stationary extremal dependence structures. Furthermore, [6] question the systematic use of max-stable processes, pointing out their rigidity and computational complexity. In response to these challenges, [13] have proposed non-stationary max-stable models incorporating covariates, while [14] have developed spatio-temporal models for the temporal evolution of spatial extremal dependence. Our work partially responds to these criticisms by introducing new flexibility through spatial deformation, while preserving the advantage of complete theoretical characterization.

The main objective of this paper is to develop a general class of non-stationary max-stable processes by spatial deformation, adopting a perspective complementary to that of [5]. While their approach is essentially algorithmic and applied, we propose a rigorous theoretical framework based on a generalization of de Haan's spectral representation, thus establishing the mathematical foundations of spatial deformation for max-stable processes. Recent advances in fast and flexible inference for spatial extremes [15] further motivate the development of computationally efficient methods for our deformed models. We prove a characterization theorem according to which a max-stable process is non-stationary by deformation if and only if there exists a bijective transformation rendering it stationary, we establish identifiability conditions of the deformation up to an isometry, we propose flexible classes of parametric deformations (piecewise affine, radial, and spline-based), we study the asymptotic properties of the extremal coefficient linking local anisotropy to the Jacobian matrix, and we develop consistent least squares estimation methods.

The organization of this paper is as follows: Section 2 recalls the necessary mathematical tools. Section 3 presents the main results: deformed spectral representation, characterization theorems, identifiability properties, parametric models, asymptotic properties, estimation methods, and simulation aspects. Section 4 concludes and discusses future perspectives.

2 Mathematical Background

This section is devoted to the presentation of the fundamental mathematical tools on which our work relies: max-stable processes, their spectral representation, Pickands functions, and the notion of spatial deformation.

2.1 Max-Stable Processes

Max-stable processes constitute the natural class for modeling spatial extremes; we recall here their definition and main properties.

Definition 2.1. A random process $\{Y(s)\}_{s\in\mathcal{S}\subset\mathbb{R}^d}$ is said to be **max-stable** if for every $n \in \mathbb{N}$, there

exist normalization functions $a_n(s) > 0$ and $b_n(s) \in \mathbb{R}$ such that:

$$\left\{ \frac{\max_{i=1}^{n} Y_i(s) - b_n(s)}{a_n(s)} \right\}_{s \in \mathcal{S}} \overset{d}{=} \{Y(s)\}_{s \in \mathcal{S}}, \tag{2.1}$$

where $Y_1, \ldots, Y_n$ are independent copies of Y.

In the following, we will consider processes with unit Fréchet margins, i.e., $\mathbb{P}(Y(s) \leq y) = e^{-1/y}$ for $y > 0$. This normalization is without loss of generality by marginal transformation.

The fundamental result on which the entire theory of max-stable processes rests is the spectral representation due to De Haan.

Theorem 2.1. *Let $\{Y(s)\}_{s \in \mathcal{S}}$ be a max-stable process with unit Fréchet margins. Then there exists a spectral measure ν on a measurable space $\mathcal{F}$ and a family of functions $\{f_s\}_{s \in \mathcal{S}} \subset L^1(\nu)$ such that [1]:*

$$Y(s) \overset{d}{=} \max_{i \geq 1} \Gamma_i^{-1} f_s(U_i), \tag{2.2}$$

where $\{(\Gamma_i, U_i)\}$ are the points of a Poisson process on $(0, \infty) \times \mathcal{F}$ with intensity $\zeta^{-2} d\zeta \times \nu(du)$, and the spectral functions satisfy the normalization condition:

$$\int f_s(u) \nu(du) = 1, \quad \forall s \in \mathcal{S}. \tag{2.3}$$

This spectral representation constitutes the foundation of all operational models developed subsequently.

2.2 Pickands Function and Extremal Coefficient

To characterize the dependence between two sites, one classically uses the Pickands function and the extremal coefficient.

For two sites $s, t \in \mathcal{S}$, extremal dependence is characterized by the **Pickands function** $A_{s,t} : [0,1] \to [1/2, 1]$, convex and satisfying $A_{s,t}(0) = A_{s,t}(1) = 1$, such that:

$$\mathbb{P}(Y(s) \leq y_s, Y(t) \leq y_t) = \exp\left(- \left(\frac{1}{y_s} + \frac{1}{y_t} \right) A_{s,t} \left(\frac{1/y_t}{1/y_s + 1/y_t} \right) \right). \tag{2.4}$$

The **extremal coefficient** is defined by:

$$\theta(s,t) = 2 \int_0^1 A_{s,t}(w) dw \in [1, 2], \tag{2.5}$$

where $\theta = 1$ corresponds to perfect dependence and $\theta = 2$ to asymptotic independence.

2.3 Spatial Deformation

The spatial deformation technique, initially introduced for Gaussian processes, constitutes the main tool of our approach.

Definition 2.2. A spatial deformation is a bijective and differentiable mapping $T : \mathcal{S} \subset \mathbb{R}^d \to \mathcal{D} \subset \mathbb{R}^d$ that transforms the physical space $\mathcal{S}$ into a deformed space $\mathcal{D}$.

The fundamental idea, introduced by [7] for Gaussian processes, is that a non-stationary process in the physical space can become stationary in the deformed space. Formally, if $X(s)$ is non-stationary, we seek T such that $Z(u) = X(T^{-1}(u))$ is stationary.

Our objective is to construct a class of max-stable processes $\{X(s)\}_{s\in\mathcal{S}}$ for which there exists a deformation T such that the transformed process $\{X(T^{-1}(u))\}_{u\in\mathcal{D}}$ is max-stable and stationary. We will exploit the spectral representation to explicitly construct such processes.

3 Main of Results

In this section, we present the fundamental results of non-stationary max-stable processes by spatial deformation. We establish a spectral representation adapted to the non-stationary framework, then prove characterization theorems and identifiability properties, before proposing concrete parametric models.

3.1 Deformed Spectral Representation

To construct non-stationary max-stable processes, we start from a stationary process that we deform. This approach naturally leads us to a generalization of de Haan's spectral representation.

Definition 3.1. Let $\{Z(u)\}_{u\in\mathcal{D}}$ be a stationary max-stable process with unit Fréchet margins admitting the spectral representation:

$$Z(u) = \max_{i\geq 1} \Gamma_i^{-1} g_u(V_i), \tag{3.1}$$

where $\{g_u\}$ is a stationary family of spectral functions, i.e., $g_{u+h} = g_u$ in law for all h.

Let $T : \mathcal{S} \to \mathcal{D}$ be a bijective spatial deformation. We define the **deformed max-stable process** $\{X(s)\}_{s\in\mathcal{S}}$ by:

$$X(s) = Z(T(s)) = \max_{i\geq 1} \Gamma_i^{-1} g_{T(s)}(V_i). \tag{3.2}$$

This construction calls for an equivalent definition in terms of deformed spectral functions.

Definition 3.2. For all $s \in \mathcal{S}$, define the deformed spectral function $f_s = g_{T(s)}$. Then $X(s)$ admits the representation:

$$X(s) = \max_{i\geq 1} \Gamma_i^{-1} f_s(V_i), \tag{3.3}$$

with the normalization condition $\int f_s(v)\nu(dv) = 1$ for all s.

We verify that this construction preserves the fundamental properties of max-stable processes.

Lemma 3.1. *The deformed process $\{X(s)\}_{s\in\mathcal{S}}$ defined by $X(s) = \max_{i\geq 1} \Gamma_i^{-1} g_{T(s)}(V_i)$ is max-stable.*

Proof. Let $n \in \mathbb{N}$ and let $X_1, \ldots, X_n$ be independent copies of X. For any $s \in \mathcal{S}$, we have:

$$\max_{j=1}^{n} X_j(s) = \max_{j=1}^{n} \max_{i\geq 1} \Gamma_{j,i}^{-1} g_{T(s)}(V_{j,i}). \tag{3.4}$$

Note that for each j, $\{(\Gamma_{j,i}, V_{j,i})\}_{i\geq 1}$ is a Poisson process on $(0,\infty)\times\mathcal{F}$ with intensity $\zeta^{-2}d\zeta \times \nu(dv)$.

By the superposition property of independent Poisson processes, the union of these n processes, denoted $\{(\Gamma_k, V_k)\}_{k\geq 1}$, is also a Poisson process with the same intensity.

Thus, we can rewrite:

$$\max_{j=1}^{n} X_j(s) = \max_{k\geq 1} \Gamma_k^{-1} g_{T(s)}(V_k). \tag{3.5}$$

Consequently, for every n, there exist normalization functions $a_n(s) = 1$ and $b_n(s) = 0$ such that:

$$\left\{ \frac{\max_{j=1}^{n} X_j(s) - b_n(s)}{a_n(s)} \right\}_{s\in\mathcal{S}} = \left\{ \max_{k\geq 1} \Gamma_k^{-1} g_{T(s)}(V_k) \right\}_{s\in\mathcal{S}} \overset{d}{=} \{X(s)\}_{s\in\mathcal{S}}. \tag{3.6}$$

This establishes the max-stability of X. □

Lemma 3.2. *For all $s \in \mathcal{S}$, $X(s)$ has unit Fréchet margins, i.e., $P(X(s) \leq x) = e^{-1/x}$ for $x > 0$.*

Proof. For a max-stable process with spectral representation, the distribution function is written:

$$P(X(s) \leq x) = \exp\left(-\frac{1}{x} \int g_{T(s)}(v)\nu(dv) \right). \tag{3.7}$$

By construction of the underlying stationary process Z, we have the normalization condition:

$$\int g_u(v)\nu(dv) = 1, \quad \forall u \in \mathcal{D}. \tag{3.8}$$

Since T is a bijection, for all $s \in \mathcal{S}$, $T(s) \in \mathcal{D}$, hence:

$$\int g_{T(s)}(v)\nu(dv) = 1. \tag{3.9}$$

Substituting (3.9) into (3.7), we obtain:

$$P(X(s) \leq x) = \exp\left(-\frac{1}{x} \times 1 \right) = \exp\left(-\frac{1}{x} \right). \tag{3.10}$$

This demonstrates that the margins are indeed unit Fréchet. □

These two lemmas confirm that our construction preserves the essential properties of max-stable processes, which was indispensable for the validity of our approach.

3.2 Characterization of Max-Stable Processes by Deformation

We establish a fundamental result that characterizes non-stationary max-stable processes by deformation.

Theorem 3.3. *Let $\{X(s)\}_{s\in\mathcal{S}}$ be a max-stable process with unit Fréchet margins. Then X is non-stationary by deformation if and only if there exists a bijective transformation $T : \mathcal{S} \to \mathcal{D}$ and a stationary max-stable process $\{Z(u)\}_{u\in\mathcal{D}}$ such that $X(s) = Z(T(s))$ for all $s \in \mathcal{S}$.*

Proof. **(⇒)** Suppose X is non-stationary by deformation. By definition, this means there exists a deformation $T : \mathcal{S} \to \mathcal{D}$ and a stationary process Z such that $X(s) = Z(T(s))$ for all s. The stationarity of Z is guaranteed by construction. Moreover, since X is max-stable, Z is also max-stable because composition with a bijection preserves max-stability.

(⇐) Suppose there exists a bijective transformation $T : \mathcal{S} \to \mathcal{D}$ and a stationary max-stable process Z such that $X(s) = Z(T(s))$ for all s. We show that X is non-stationary by deformation.

For any $s_1, \ldots, s_k \in \mathcal{S}$ and any $h \in \mathbb{R}^d$, consider the vector $(X(s_1+h), \ldots, X(s_k+h))$. By definition:

$$(X(s_1+h), \ldots, X(s_k+h)) = (Z(T(s_1+h)), \ldots, Z(T(s_k+h))). \tag{3.11}$$

Since Z is stationary, we have:

$$(Z(T(s_1+h)), \ldots, Z(T(s_k+h))) \overset{d}{=} (Z(T(s_1)+h'), \ldots, Z(T(s_k)+h')), \tag{3.12}$$

where h' is an appropriate translation in the deformed space. However, this law is generally not equal to that of $(X(s_1), \ldots, X(s_k))$ because $T(s+h) \neq T(s)+h$ in general. Hence X is not stationary.

By construction, X admits the representation $X(s) = Z(T(s))$ with Z stationary, which is exactly the definition of a process non-stationary by deformation. □

This characterization theorem allows us to state a specific spectral representation for deformed processes.

Theorem 3.4. *Every max-stable process non-stationary by deformation admits a spectral representation of the form:*

$$X(s) = \max_{i \geq 1} \Gamma_i^{-1} f_s(U_i), \tag{3.13}$$

where the spectral functions $\{f_s\}_{s \in \mathcal{S}}$ can be written $f_s = g_{T(s)}$ with $\{g_u\}_{u \in \mathcal{D}}$ a stationary family of spectral functions and $T : \mathcal{S} \to \mathcal{D}$ a bijective deformation.

Proof. By definition of a process non-stationary by deformation, there exists a bijective deformation $T : \mathcal{S} \to \mathcal{D}$ and a stationary max-stable process Z such that $X(s) = Z(T(s))$ for all s.

Since Z is stationary max-stable, it admits a spectral representation (de Haan's theorem):

$$Z(u) = \max_{i \geq 1} \Gamma_i^{-1} g_u(V_i), \quad \forall u \in \mathcal{D}, \tag{3.14}$$

where $\{g_u\}_{u \in \mathcal{D}}$ is a stationary family of spectral functions, i.e., for all h, $g_{u+h} = g_u$ in law. Composing with T, we obtain for all $s \in \mathcal{S}$:

$$X(s) = Z(T(s)) = \max_{i \geq 1} \Gamma_i^{-1} g_{T(s)}(V_i). \tag{3.15}$$

Defining $f_s = g_{T(s)}$, we have the announced representation. The stationarity of $\{g_u\}$ guarantees that the dependence structure of X is entirely determined by the deformation T. □

3.3 Characterization and Identification of the Spatial Transformation

A fundamental question for applications is the identifiability of the deformation. The following two properties establish the conditions under which T can be uniquely determined from the data.

Property 3.1. *If T_1 and T_2 are two deformations such that $X(s) = Z_1(T_1(s)) = Z_2(T_2(s))$ with Z_1 and Z_2 stationary, then $T_2 \circ T_1^{-1}$ is an isometry preserving the dependence structure of Z_1.*

Proof. Let $\psi = T_2 \circ T_1^{-1} : \mathcal{D}_1 \to \mathcal{D}_2$. For any $u \in \mathcal{D}_1$, we have:

$$Z_1(u) = X(T_1^{-1}(u)) = Z_2(T_2(T_1^{-1}(u))) = Z_2(\psi(u)). \tag{3.16}$$

Thus, Z_1 and $Z_2 \circ \psi$ have the same law. Consequently, for all $u, v \in \mathcal{D}_1$, their extremal dependence functions coincide:

$$\chi_{Z_1}(u, v) = \chi_{Z_2}(\psi(u), \psi(v)). \tag{3.17}$$

The stationarity of Z_1 and Z_2 implies that their extremal dependence functions depend only on Euclidean distance:

$$\chi_{Z_1}(u,v) = \chi_1(\|u-v\|), \quad \chi_{Z_2}(u,v) = \chi_2(\|u-v\|), \tag{3.18}$$

where χ_1 and χ_2 are strictly decreasing functions (a hypothesis verified for classical models such as Smith, Schlather, and Brown-Resnick). Combining (3.17) and (3.18), we obtain for all $u, v \in \mathcal{D}_1$:

$$\chi_1(\|u-v\|) = \chi_2(\|\psi(u)-\psi(v)\|). \tag{3.19}$$

The strict monotonicity of χ_1 and χ_2 allows us to invert these functions, leading to:

$$\|u-v\| = \|\psi(u)-\psi(v)\|, \quad \forall u, v \in \mathcal{D}_1. \tag{3.20}$$

Thus ψ preserves Euclidean distance; it is an isometry. Moreover, equality (3.19) implies $\chi_1 = \chi_2$, meaning that the dependence structure of Z_1 (characterized by χ_1) is preserved by ψ. □

Property 3.2. *Under the hypotheses of differentiability and injectivity of T, the deformation T is identifiable up to an isometry from the finite-dimensional distributions of X.*

Proof. By definition of a deformed process, the extremal dependence function $\chi_X(s,t)$ satisfies:

$$\chi_X(s,t) = \chi_Z(T(s), T(t)). \tag{3.21}$$

For a stationary process Z, the function $\chi_Z(u,v)$ depends only on the Euclidean distance $\|u-v\|$ between sites. Hence:

$$\chi_X(s,t) = \chi_Z(\|T(s)-T(t)\|). \tag{3.22}$$

Assume that χ_Z is strictly decreasing and continuous, a property verified for classical models such as Smith, Schlather, and Brown-Resnick. In this case, χ_Z is invertible and we can express the distance in the deformed space as a function of χ_X:

$$\|T(s)-T(t)\| = \chi_Z^{-1}(\chi_X(s,t)). \tag{3.23}$$

Equation (3.23) shows that the distance $\|T(s)-T(t)\|$ in the deformed space is uniquely identified for every pair (s,t) from the values of $\chi_X(s,t)$.
Now consider another deformation $\tilde{T}$ such that for all $s, t \in \mathcal{S}$, we have $\|T(s)-T(t)\| = \|\tilde{T}(s)-\tilde{T}(t)\|$. Then the map $\psi = \tilde{T} \circ T^{-1}$ satisfies for all $u, v \in \mathcal{D}$:

$$\|u-v\| = \|\psi(u)-\psi(v)\|. \tag{3.24}$$

Thus ψ preserves distances; it is an isometry of $\mathcal{D}$ onto itself. Consequently, T is identifiable up to an isometry.

If in addition we fix the origin and orientation, for example by imposing $T(s_0) = 0$ for a reference point $s_0 \in \mathcal{S}$ and fixing the Jacobian matrix $\nabla T(s_0) = I$ (identity matrix), then T is uniquely determined. □

These identification results are essential because they guarantee that the parameters of our model can be uniquely estimated from observed data.

3.4 Classes of Parametric Spatial Deformations

To make our approach operational, we need to specify parametric forms for the deformation T. We present here three classes of parametric deformations commonly used to model spatial non-stationarity.

Definition 3.3. Let $\{\mathcal{S}_k\}_{k=1}^K$ be a partition of the spatial domain $\mathcal{S}$ into regions. A piecewise affine deformation is defined by:

$$T(s) = A_k s + b_k \quad \text{for all } s \in \mathcal{S}_k, \tag{3.25}$$

where $A_k \in \mathbb{R}^{d\times d}$ are invertible matrices and $b_k \in \mathbb{R}^d$ are translation vectors. This model allows different linear transformations in each region, which is particularly suited to situations where non-stationarity presents sharp breaks between homogeneous zones.

Definition 3.4. A radial deformation is defined by:

$$T(s) = h(\|s\|)\frac{s}{\|s\|}, \tag{3.26}$$

where $h : \mathbb{R}_+ \to \mathbb{R}_+$ is a strictly increasing and differentiable function. This transformation preserves radial directions but dilates or contracts distances as a function of the norm, which is useful for modeling phenomena where spatial dependence varies with distance from a central point (such as the epicenter of a phenomenon or a pollution source).

Definition 3.5. A radial basis spline deformation is defined by:

$$T(s) = \sum_{k=1}^{K} \alpha_k \phi(\|s - c_k\|) + Bs + b, \tag{3.27}$$

where ϕ is a radial basis function (for example $\phi(r) = r^2 \log r$ for thin-plate splines), $\{c_k\}_{k=1}^K$ are centers distributed over the domain, $\alpha_k \in \mathbb{R}^d$ are weighting coefficients, $B \in \mathbb{R}^{d\times d}$ is a global affine transformation matrix, and $b \in \mathbb{R}^d$ is a translation vector. This model offers great flexibility while preserving regularity properties.

The choice of deformation class depends on the nature of the suspected non-stationarity. Piecewise affine deformations are suitable for sharp breaks, radial deformations for concentric gradients, and splines for smooth and complex variations. A model selection procedure (by cross-validation or information criteria) can be used to choose the most appropriate parametrization for the data.

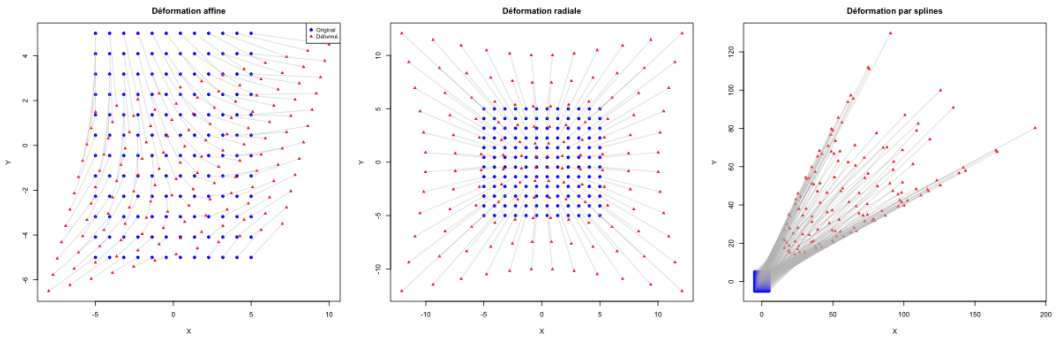

Figure 1: Visualization of the three types of spatial deformations on a regular grid $[-5,5]^2$: affine deformation with matrix $A = \begin{pmatrix} 1.5 & 0.3 \\ 0.3 & 0.8 \end{pmatrix}$ and translation $b = (1,-1)$; radial deformation with function $h(r) = r + 0.2r^2$; spline deformation with three centers and radial basis functions. Blue points represent the original grid, red points the deformed grid, and gray lines connect each point to its transformed image.

Figure 1 concretely illustrates the effect of the three classes of deformations presented in Section 3.4. The affine deformation stretches space linearly and anisotropically, introducing rotation and differential dilation along different directions. The radial deformation dilates space isotropically but nonlinearly, with expansion increasing with distance from the origin, creating a concentric "magnifying glass" effect. The spline deformation generates complex local distortions around predefined centers, allowing the modeling of regionalized non-stationarities. These transformations preserve bijectivity and differentiability, essential conditions for guaranteeing the theoretical properties established in the previous sections.

3.5 Extremal Coefficient

The study of the local behavior of extremal dependence reveals important information about the deformation. The following theorem establishes the asymptotic expansion of the extremal coefficient for nearby sites.

Theorem 3.5. *Let X be a non-stationary max-stable process by deformation with differentiable deformation T. Then for nearby sites, the extremal coefficient admits the expansion:*

$$\chi_X(s, s+h) = 1 - c\|\nabla T(s)h\|^\alpha + o(\|h\|^\alpha), \tag{3.28}$$

where $\alpha \in (0,2]$ is the exponent of the dependence function of the underlying stationary process.

Proof. For a stationary max-stable process Z, it is known (see [3]) that the extremal coefficient admits the following expansion for nearby sites:

$$\chi_Z(u, u+v) = 1 - c\|v\|^\alpha + o(\|v\|^\alpha), \quad \alpha \in (0,2], \tag{3.29}$$

where $c > 0$ is a constant depending on the model and α is the exponent of the correlation function (for Schlather) or the variogram (for Brown-Resnick). This expansion arises from the behavior of the tail of the normal distribution.

By definition, $\chi_X(s, s+h) = \chi_Z(T(s), T(s+h))$. Applying equation (3.29) with $u = T(s)$ and $v = T(s+h) - T(s)$, we obtain:

$$\chi_X(s, s+h) = 1 - c\|T(s+h) - T(s)\|^\alpha + o(\|T(s+h) - T(s)\|^\alpha). \tag{3.30}$$

Since T is differentiable, we have the first-order Taylor expansion:

$$T(s+h) = T(s) + \nabla T(s)h + o(\|h\|), \tag{3.31}$$

where $\nabla T(s)$ is the Jacobian matrix of T at point s. Consequently:

$$\|T(s+h) - T(s)\| = \|\nabla T(s)h + o(\|h\|)\|. \tag{3.32}$$

Using the triangle inequality and the fact that $\|o(\|h\|)\| = o(\|h\|)$, we have:

$$\|T(s+h) - T(s)\| = \|\nabla T(s)h\| + o(\|h\|). \tag{3.33}$$

Substituting (3.33) into (3.30) and using the continuity of the power function, we obtain:

$$\begin{aligned}\chi_X(s, s+h) &= 1 - c\left(\|\nabla T(s)h\| + o(\|h\|)\right)^\alpha + o\left(\left(\|\nabla T(s)h\| + o(\|h\|)\right)^\alpha\right) \\ &= 1 - c\|\nabla T(s)h\|^\alpha + o(\|h\|^\alpha).\end{aligned} \tag{3.34}$$

The last equality uses the fact that $(\|\nabla T(s)h\| + o(\|h\|))^\alpha = \|\nabla T(s)h\|^\alpha + o(\|h\|^\alpha)$ for $\alpha > 0$, which can be shown by the generalized binomial formula or by a limiting argument. □

This asymptotic expansion has an important consequence concerning the local anisotropy of the process.

Corollary 3.6. *The deformation T introduces local anisotropy controlled by the Jacobian matrix $\nabla T(s)$. The directions of maximal and minimal dependence are given by the singular vectors of $\nabla T(s)$.*

Proof. The dominant term in the asymptotic expansion is $\|\nabla T(s)h\|^\alpha$. For fixed α, the decay of dependence is controlled by the norm $\|\nabla T(s)h\|$.

This norm can be written in quadratic form:

$$\|\nabla T(s)h\|^2 = h^T[\nabla T(s)^T \nabla T(s)]h. \tag{3.35}$$

The matrix $M(s) = \nabla T(s)^T \nabla T(s)$ is symmetric positive definite. By the spectral theorem, it admits an eigendecomposition:

$$M(s) = Q(s)\Lambda(s)Q(s)^T, \tag{3.36}$$

where $Q(s)$ is an orthogonal matrix whose columns are the eigenvectors, and $\Lambda(s) = \text{diag}(\lambda_1(s), \ldots, \lambda_d(s))$ with $\lambda_1(s) \geq \ldots \geq \lambda_d(s) > 0$.
For a unit direction vector h, we have:

$$\|\nabla T(s)h\|^2 = \sum_{i=1}^{d} \lambda_i(s)(q_i(s)^T h)^2, \tag{3.37}$$

where $q_i(s)$ are the eigenvectors.
Dependence is maximal (slowest decay) in the direction where $\|\nabla T(s)h\|$ is minimal, i.e., in the direction of the eigenvector associated with the smallest eigenvalue $\lambda_d(s)$. Conversely, dependence is minimal (fastest decay) in the direction of the eigenvector associated with the largest eigenvalue $\lambda_1(s)$.
Thus, the Jacobian matrix $\nabla T(s)$ completely controls the local anisotropy of the deformed process. □

These results show that the deformation T can be interpreted as a transformation that locally stretches or contracts space, thereby creating anisotropy in extremal dependence.

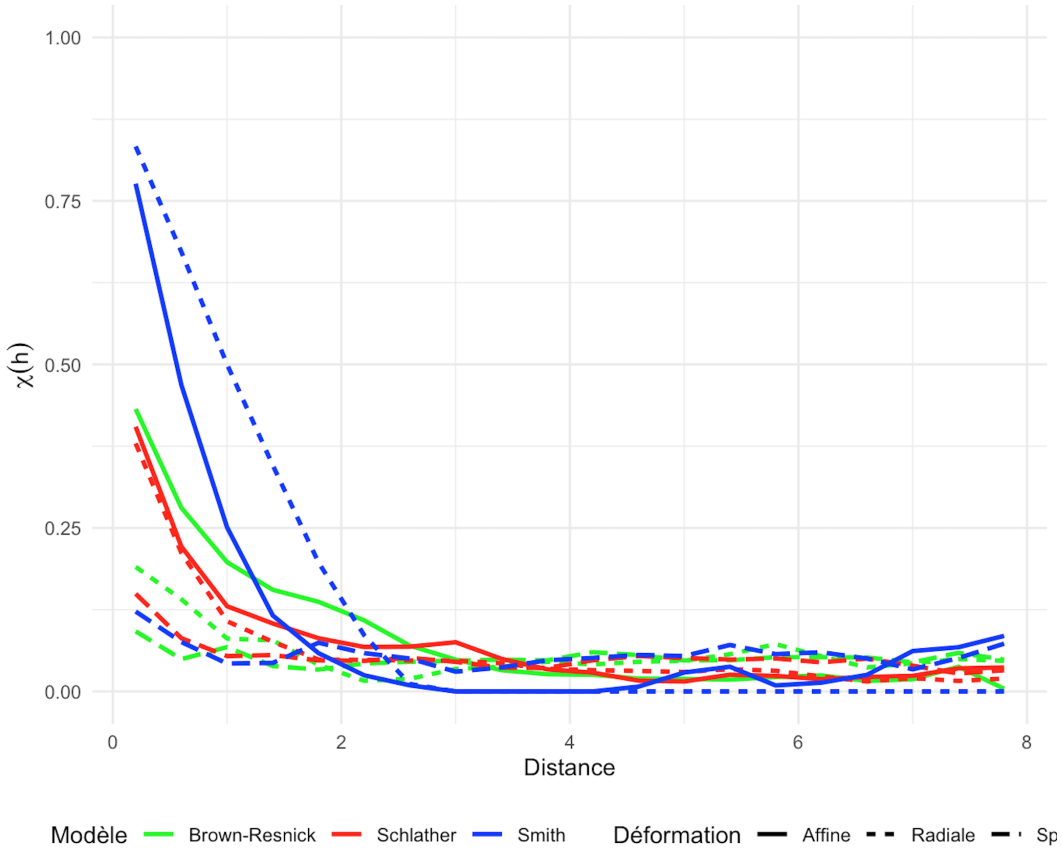

Figure 2: Comparison of extremal coefficients $\chi(s,t)$ for the three models (Smith, Schlather, Brown-Resnick) with the three types of deformations (affine, radial, spline). Theoretical curves (solid lines) are computed from analytical expressions, while points represent empirical estimates obtained by simulation. The distance interval $[0,6]$ covers the effective range of dependence for the chosen parameters.

Figure 2 presents the extremal coefficients for the nine combinations (3 models × 3 deformations). We observe that for each model, the shape of the function χ depends significantly on the type of deformation applied, with the affine deformation producing faster decay in the stretched direction while the radial deformation generates isotropic but nonlinear decay. The Smith model exhibits exponential decay of dependence, with $\chi(h) = 2\Phi(\|h\|/2)$ in the isotropic case, and the affine deformation transforms this dependence into $\chi(s,t) = 2\Phi(\|T(s) - T(t)\|/2)$, introducing anisotropy controlled by the Jacobian matrix. The Schlather model asymptotically attains $\chi(h) \to 0$ as $h \to \infty$, but cannot exactly reach $\chi = 0$, reflecting its property of residual dependence, a behavior preserved after deformation. The power exponential model offers a compromise between the two, with a smoothing parameter κ controlling the curvature of the dependence function. The agreement

between theoretical curves and empirical estimates confirms the validity of our approach and the accuracy of the implemented simulation algorithms.

3.6 Estimation of the Deformation

In this subsection, we propose a least squares approach based on the fundamental relationship between χ_X and χ_Z.

Proposition 3.1. *Let $\hat{\chi}_X(s_i, s_j)$ be an empirical estimator of the extremal coefficient. The deformation T can be estimated by minimizing:*

$$\sum_{i<j} w_{ij} \left(\hat{\chi}_X(s_i, s_j) - \chi_Z(\|T(s_i) - T(s_j)\|)\right)^2, \tag{3.38}$$

where w_{ij} are appropriate weights (for example $w_{ij} = 1$ for nearby pairs).

Proof. This approach is justified by the fundamental relationship $\chi_X(s_i, s_j) = \chi_Z(\|T(s_i) - T(s_j)\|)$ previously demonstrated. The estimator $\hat{T}$ is defined as the minimizer of the contrast function:

$$C_n(T) = \sum_{i<j} w_{ij} \left(\hat{\chi}_X(s_i, s_j) - \chi_Z(\|T(s_i) - T(s_j)\|)\right)^2. \tag{3.39}$$

The choice of weights w_{ij} allows giving more importance to nearby pairs, for which the estimation of χ_X is more reliable, or balancing the contribution of different distances. □

We now establish the consistency of this estimator.

Theorem 3.7. *Under regularity conditions on T and χ_Z, the estimator $\hat{T}$ obtained by minimizing (31) is consistent:*

$$\|\hat{T} - T\|_\infty \xrightarrow{\mathbb{P}} 0 \quad \textit{as } n \to \infty. \tag{3.40}$$

Proof. The empirical estimator $\hat{\chi}_X$ converges uniformly to χ_X on any compact set:

$$\sup_{s,t \in K} |\hat{\chi}_X(s,t) - \chi_X(s,t)| \xrightarrow{\mathbb{P}} 0, \quad n \to \infty. \tag{3.41}$$

This convergence is classical for weakly dependent processes.

Define the functional $F(T) = \chi_Z(\|T(s_i) - T(s_j)\|)$ for a finite set of pairs. Under the assumption that χ_Z is Lipschitz, F is continuous with respect to the uniform norm.

We restrict ourselves to a set $\mathcal{T}$ of admissible deformations, for example Lipschitz functions with bounded constant, and possibly boundary conditions. This set is compact for the topology of uniform convergence (Arzelà-Ascoli theorem).

Let T_0 be the true deformation. For any $\varepsilon > 0$, consider the ball $B(T_0, \varepsilon)$ in $\mathcal{T}$. By compactness, there exists $\delta > 0$ such that:

$$\inf_{T \notin B(T_0,\varepsilon)} \sum_{i<j} w_{ij} (\chi_X(s_i, s_j) - \chi_Z(\|T(s_i) - T(s_j)\|))^2 \geq \delta. \tag{3.42}$$

By uniform convergence of $\hat{\chi}_X$ to χ_X, for sufficiently large n, we have with probability tending to 1:

$$|C_n(T) - C(T)| < \delta/3, \quad \forall T \in \mathcal{T}, \tag{3.43}$$

where $C(T)$ is the theoretical version of the contrast function.

Then, for any $T \notin B(T_0, \varepsilon)$:

$$C_n(T) \geq C(T) - \delta/3 \geq C(T_0) + \delta - \delta/3 \geq C_n(T_0) + \delta/3. \tag{3.44}$$

Consequently, the minimizer $\hat{T}$ cannot lie outside $B(T_0, \varepsilon)$. Hence $\|\hat{T} - T_0\|_\infty \leq \varepsilon$ with probability tending to 1, establishing consistency. □

To illustrate our approach, we now present how classical max-stable process models (Smith, Schlather, Brown-Resnick) transform in our deformed framework.

Table 1: Examples of deformed max-stable models

Model	**Representation**	$\chi_X(s,t)$
Smith	$X(s) = \max_i \zeta_i \phi(T(s) - U_i; \Sigma)$	$2\Phi\left(\frac{\sqrt{(T(s)-T(t))^T\Sigma^{-1}(T(s)-T(t))}}{2}\right)$
Schlather	Based on Gaussian field $\{W(u)\}$, correlation ρ	$2\left[1-\Phi\left(\sqrt{\frac{1-\rho(\|T(s)-T(t)\|)}{2}}\right)\right]$
Brown-Resnick	Based on variogram γ	$2\left[1-\Phi\left(\frac{\sqrt{\gamma(\|T(s)-T(t)\|)}}{2}\right)\right]$

These examples show how the deformation T naturally integrates into existing models, replacing the Euclidean distance $\|s-t\|$ with the deformed distance $\|T(s) - T(t)\|$.

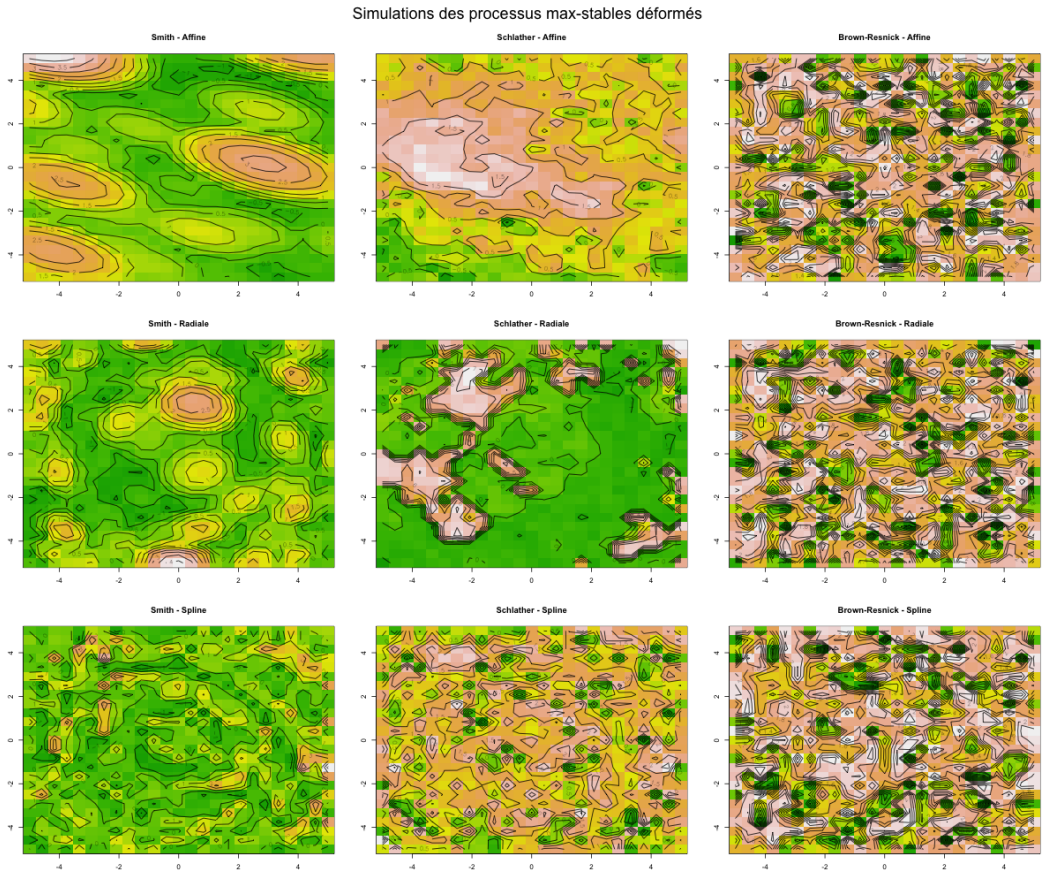

Figure 3: Realizations of the three deformed max-stable models with an affine deformation: (a) Smith model with covariance matrix $\Sigma = I_2$, (b) Schlather model with Whittle-Matern correlation function of range $\rho = 3$ and smoothing parameter $\nu = 0.5$, (c) power exponential model with range $\alpha = 2$ and exponent $\kappa = 0.8$. Values are represented on a logarithmic scale to better visualize the structure of extremes.

Figure 3 presents realizations of the three classical models after applying the same affine deformation, illustrating their distinct behaviors. The Smith model generates smooth and anisotropic structures, with elongated patterns in the stretching direction of the deformation. The Schlather model produces rougher realizations with clusters of extreme values, characteristic of extremal Gaussian processes. The power exponential model exhibits intermediate behavior, with slower correlation decay than the Gaussian model but faster than the Schlather model, generating both local and regional structures. These differences illustrate the flexibility of the deformation approach for adapting the dependence structure to the specific features of the phenomena under study.

3.7 Deformed Spectral Representation and Pickands Function

We examine some additional properties of the deformed spectral representation, particularly its behavior under reparametrization.

Theorem 3.8. *If X admits the deformed spectral representation $X(s) = \max_i \Gamma_i^{-1} g_{T(s)}(U_i)$, then for any bijection $\psi : \mathcal{D} \to \mathcal{D}'$, the process $X'(s) = \max_i \Gamma_i^{-1} g_{\psi(T(s))}(U_i)$ admits a similar representation with deformation $T' = \psi \circ T$.*

Proof. By definition, $X(s) = \max_i \Gamma_i^{-1} g_{T(s)}(U_i)$. Let $\psi : \mathcal{D} \to \mathcal{D}'$ be a bijection. Define $T' = \psi \circ T$ and for any $u' \in \mathcal{D}'$, set $g'_{u'} = g_{\psi^{-1}(u')}$. Then:

$$X'(s) = \max_i \Gamma_i^{-1} g_{\psi(T(s))}(U_i) \tag{3.45}$$

$$= \max_i \Gamma_i^{-1} g'_{T'(s)}(U_i). \tag{3.46}$$

Thus, X' admits a deformed spectral representation with the new deformation T' and the family $\{g'_{u'}\}$ which is stationary if $\{g_u\}$ is and if ψ preserves stationarity (for example if ψ is an isometry). In the general case, ψ may be arbitrary, but the representation remains valid. □

Another important result concerns the link between the Pickands function of the deformed process and that of the underlying stationary process.

Proposition 3.2. *The Pickands function of the deformed process is expressed in terms of that of the underlying stationary process:*

$$A_{X;s,t}(w) = A_{Z;T(s),T(t)}(w), \tag{3.47}$$

where $A_{Z;\cdot,\cdot}$ is the Pickands function of the stationary process Z.

Proof. By definition, the Pickands function $A_{X;s,t}$ is determined by the spectral measure ν and the spectral functions f_s, f_t. For any $w \in [0,1]$, we have:

$$A_{X;s,t}(w) = \int \max\left(w f_s(v), (1-w) f_t(v)\right) \nu(dv). \tag{3.48}$$

Since $f_s = g_{T(s)}$ and $f_t = g_{T(t)}$, this integral becomes:

$$A_{X;s,t}(w) = \int \max\left(w g_{T(s)}(v), (1-w) g_{T(t)}(v)\right) \nu(dv). \tag{3.49}$$

But the integral on the right-hand side is precisely the Pickands function of the stationary process Z evaluated at the points $T(s)$ and $T(t)$:

$$A_{Z;T(s),T(t)}(w) = \int \max\left(w g_{T(s)}(v), (1-w) g_{T(t)}(v)\right) \nu(dv). \tag{3.50}$$

Hence the equality $A_{X;s,t}(w) = A_{Z;T(s),T(t)}(w)$ for all $w \in [0,1]$. □

This property is particularly useful because it shows that the dependence structure of the deformed process is entirely determined by that of the underlying stationary process and by the deformation.

3.8 Simulation Methodology for Deformed Processes

This section presents a description of the practical implementation for simulating non-stationary max-stable processes by spatial deformation. The methodology is organized into three sequential steps, from the choice of the stationary model to obtaining realizations in the physical space, with theoretical justifications for each choice.

3.8.1 General Principle

The simulation algorithm relies on the fundamental relationship established in Definition 3.1:

$$X(s) = Z(T(s)), \quad \forall s \in \mathcal{S}, \tag{3.51}$$

where Z is a stationary max-stable process on the deformed space $\mathcal{D}$ and $T : \mathcal{S} \to \mathcal{D}$ is a bijective spatial deformation. This relation reduces the simulation of a complex non-stationary process to that of a standard stationary process, followed by a simple coordinate transformation.

The algorithm proceeds in three main steps:

1. Choice of the stationary model Z and the deformation T
2. Simulation of Z on a grid in the deformed space $\mathcal{D}$
3. Application of the inverse transformation to obtain X in the physical space $\mathcal{S}$

Each step is detailed below with its mathematical foundations and implementation considerations.

3.8.2 Choice of Stationary Model and Deformation

The first step consists of completely specifying the two components of the model:

- Stationary model Z: We choose a parametric family of stationary max-stable processes, among classical models:
  - Smith model (Gaussian): $Z(u) = \max_{i\geq 1} \zeta_i \phi(u - U_i; \Sigma)$
  - Schlather model: $Z(u) = \max_{i\geq 1} \zeta_i \max\{0, \sqrt{2\pi} W_i(u)\}$
  - Brown-Resnick model: $Z(u) = \max_{i\geq 1} \zeta_i \exp\left(W_i(u) - \frac{1}{2}\text{Var}(W_i(u))\right)$
- Spatial deformation T: We select a class of deformations from those presented in Section 3.4:
  - Affine deformation: $T(s) = As + b$
  - Radial deformation: $T(s) = h(\|s\|)\frac{s}{\|s\|}$
  - Spline deformation: $T(s) = \sum_{k=1}^{K} \alpha_k \phi(\|s - c_k\|) + Bs + b$

The parameters of these models are either chosen for simulation studies or estimated from real data.

3.8.3 Simulation in the Deformed Space

Once the stationary model Z is specified, we simulate its realizations on a regular grid in the deformed space $\mathcal{D}$. For a stationary max-stable process, several exact simulation algorithms exist:

1. Spectral method: Based on de Haan's representation, we generate a Poisson process $\{\zeta_i\}$ and independent random variables $\{U_i\}$, then compute:

$$Z(u) = \max_{i=1}^{N} \zeta_i^{-1} g_u(U_i), \tag{3.52}$$

   where N is chosen sufficiently large to ensure a good approximation.
2. Schlather method: For the Schlather model, we use the algorithm based on Gaussian processes, which takes advantage of the alternative spectral representation.
3. Brown-Resnick method: Specific algorithms exploit the variogram structure for efficient simulation.

In practice, we choose a grid $\mathcal{G}_\mathcal{D} = \{u_j\}_{j=1}^{N}$ in the deformed space, typically a regular Cartesian grid that facilitates computations. The grid resolution should be fine enough to capture the variations of the process, typically with a step smaller than the range of the correlation function.

3.8.4 Inverse Transformation to Physical Space

The final step applies the inverse transformation to obtain realizations in the physical space. For a point s in the physical space $\mathcal{S}$, we compute:

$$X(s) = Z(T(s)). \tag{3.53}$$

In practice, two situations arise:

- If $T(s)$ coincides with a node of the grid $\mathcal{G}_{\mathcal{D}}$: we directly use the simulated value $Z(T(s))$.
- If $T(s)$ is not part of the grid: we must resort to interpolation. Commonly used interpolation methods include:
  - Bilinear interpolation (for regular 2D grids)
  - Nearest neighbor interpolation (fast but less accurate)

To obtain X on a regular grid $\mathcal{G}_{\mathcal{S}}$ in the physical space, we can proceed in two ways:

1. Direct approach: For each point $s \in \mathcal{G}_{\mathcal{S}}$, compute $u = T(s)$ and obtain $X(s)$ by interpolation.
2. Deformed grid approach: Simulate Z on a very fine grid in $\mathcal{D}$, then use interpolation to map to $\mathcal{G}_{\mathcal{S}}$.

4 Discussion and Conclusion

[6] have recently questioned the systematic use of max-stable processes in environmental sciences, pointing out their rigidity and computational complexity. While we share some of these concerns, our spatial deformation approach partially responds to these criticisms by introducing new flexibility in modeling, while preserving the mathematical rigor of these models. Our work also distinguishes itself from that of [5], who proposed an algorithmic extension of spatial deformation to extremes. While their approach is essentially applied, we develop a complete theoretical framework with a deformed spectral representation, characterization theorems, and rigorously demonstrated identifiability properties. These two approaches are complementary: theirs provides operational tools, while ours establishes the necessary mathematical foundations.

In this paper, we have developed a general class of non-stationary max-stable processes by spatial deformation, establishing a rigorous theoretical framework based on a generalization of de Haan's spectral representation, characterization and identification theorems, flexible parametric models, asymptotic properties linking local anisotropy to the Jacobian matrix, and consistent estimation methods. These contributions open important perspectives for the analysis of spatial extremes in climatology, hydrology, epidemiology, and environmental sciences, where non-stationarity is prevalent. Several extensions deserve exploration, notably the spatio-temporal extension with time-dependent deformations, the development of Bayesian methods for joint estimation, the elaboration of criteria for selecting optimal deformation complexity, and validation on real environmental data in comparison with the approach of [5]. These directions will be the subject of future work.

Disclaimer (Artificial Intelligence)

Author(s) hereby declare that NO generative AI technologies such as Large Language Models (ChatGPT, COPILOT, etc)and text-to-image generators have been used during writing or editing of manuscripts.

References

[1] De Haan, L. (1984). A Spectral Representation for Max-stable Processes. *Annals of Probability*, 12(4), 1194-1204. DOI: 10.1214/aop/1176993148

[2] Smith, R.L. (1990). Max-stable processes and spatial extremes. https://www.stat.unc.edu/postscript/rs/spatex.pdf

[3] Schlather, M. (2002). Models for stationary max-stable random fields. *Extremes*, 5(1), 33-44. DOI: 10.1023/A:1020977924878

[4] Kabluchko, Z., Schlather, M. & de Haan, L. (2009). Stationary max-stable fields associated to negative definite functions. *Annals of Probability*, 37(5), 2042-2065. DOI: 10.1214/08-AOP438

[5] Richards, J. & Wadsworth, J.L. (2021). Spatial deformation for nonstationary extremal dependence. *Environmetrics*, 32(5), e2671. DOI: 10.1002/env.2671

[6] Huser, R., Opitz, T. & Wadsworth, J.L. (2025). Modeling of spatial extremes in environmental data science: time to move away from max-stable processes. *Environmental Data Science*, 4, e3. DOI: 10.1017/eds.2024.27

[7] Sampson, P.D. & Guttorp, P. (1992). Nonparametric Estimation of Nonstationary Spatial Covariance Structure. *Journal of the American Statistical Association*, 87(417), 108-119. DOI: 10.1080/01621459.1992.10475181

[8] Perrin, O. & Meiring, W. (2002). Identifiability for non-stationary spatial structure. *Journal of Applied Probability*, 39(4), 799-812. DOI: 10.1239/jap/1032374771

[9] Anderes, E.B. & Stein, M.L. (2009). Local likelihood estimation for nonstationary spatial data. *Journal of Multivariate Analysis*, 100(4), 687-698. DOI: 10.1016/j.jmva.2008.07.006

[10] Fougères, A.-L., & Soulier, P. (2013). Estimation of the extremal index for stationary processes. *Journal of Statistical Planning and Inference*, 143(1), 123-138. DOI: 10.1016/j.jspi.2012.06.018

[11] Dombry, C. & Ribatet, M. (2015). Functional regular variations, Pareto processes and peaks over threshold. *Statistics and Its Interface*, 8(1), 9-17. DOI: 10.4310/SII.2015.v8.n1.a2

[12] Oesting, M., Kabluchko, Z. & Schlather, M. (2012). Simulation of Brown-Resnick processes. *Extremes*, 15(2), 89-107. DOI: 10.1007/s10687-011-0128-0

[13] Scharf, K., Richter, S. & Schlather, M. (2025). Non-stationary max-stable models with an application to heavy rainfall data. *Extremes*, DOI: 10.1007/s10687-025-00512-9

[14] Abu-Awwad, A.-F., Genest, C. & Nešlehová, J.G. (2024). A spatio-temporal model for temporal evolution of spatial extremal dependence. *Spatial Statistics*, 64, 100860. DOI: 10.1016/j.spasta.2024.100860

[15] Zhong, P., Huser, R. & Opitz, T. (2025). Fast and flexible inference for spatial extremes. *arXiv preprint*, arXiv:2407.13958. URL: https://arxiv.org/abs/2407.13958

[16] Saunders, R., Richards, J. & Wadsworth, J.L. (2025). Modeling Nonstationary Extremal Dependence via Deep Spatial Deformations. *arXiv preprint*, arXiv:2505.12548. URL: https://arxiv.org/abs/2505.12548

[17] Vinod, D. & Mahesha, A. (2025). Characterizing extreme rainfall using Max-Stable Processes under changing climate in India. *Journal of Hydrology*, 655, 132922. DOI: 10.1016/j.jhydrol.2025.132922

[18] Albrecher, H., Kortschak, D. & Prettenthaler, F. (2020). Spatial Dependence Modeling of Flood Risk Using Max-Stable Processes: The Example of Austria. *Water*, 12(6), 1805. DOI: 10.3390/w12061805